An energy-based electroelastic beam model for MEMS applications

N.E. Ligterink, M. Patrascu, P.C. Breedveld, and S. Stramigioli

Control Engineering, University Twente,
Postbus 217, 7500AE Enschede, The Netherlands

Abstract

Competent modeling of an electroelastic beam configuration is of major importance for MEMS. The MEMS motor, based on such a deformable capacitor, is driven by a voltage source. A coherent model, of limited complexity and expressed in design parameters, is derived for a step motor. The two physical regimes; the stick and non-stick, are matched, such that a smooth, single energy profile arises. The pull-in voltage, the hysteris loop, jump-back voltage, the step size, and the dissipated energies are determined as function of these design parameters. The results are compared to measurements with the μWalker.

Key words: electroelastic beam, stick, hysteresis, design parameter dependence, energy balance, pull-in voltage
PACS: 85.85.+j, 46.70.De, 46.15.Cc, 47.20.Ky

1 Introduction

A well-known effect when modeling and designing MEMS (Micro Electromechanical Systems) is that the electrostatic forces scale favorably with decreasing size [1]. At the micrometer scale, an applied voltage in a range up to $100V$ yields electrostatical forces comparable to the mechanical stiffness of the micro structure. This feature lies at the heart of an effective actuator, in our case an elastic beam with capacitance. The working principle of the elastic beam relies on a balance between electrostatic and mechanical forces. Step motors based on this principle, like the μWalker [2], are being developed for mass

Email addresses: n.e.ligterink@utwente.nl (N.E. Ligterink), m.patrascu@utwente.nl (M. Patrascu), p.c.breedveld@utwente.nl (P.C. Breedveld), s.stramigioli@utwente.nl (S. Stramigioli).

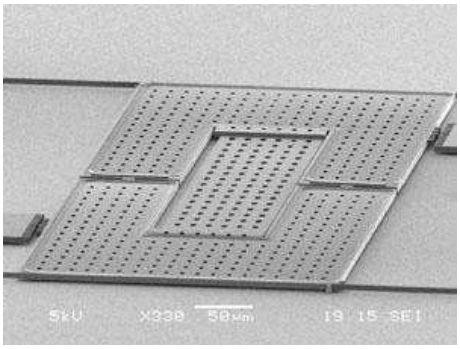

Fig. 1. One dimensional version of the μWalker used for modeling and simulation.

storage systems such as the μSPAM [3] and the Millipede [4]. As a result of electrostatic forces from an applied voltage difference, very fine and powerful steps are obtained. For the μWalker, the step size is a few tens of nm in size and by applying a high frequency of the walking cycle, velocities up to several mm/s are achievable with an accuracy in the order of $0.5nm$ per step. Figure 1 shows one realization of this micro device.

The characteristics of the beam greatly influence the properties of this device. For every applied voltage a static deformation exists. However, the corresponding dynamics is singular as above a critical pull-in voltage, the beam bending forces cannot compensate for the electrostatic forces and the beam will hit the underlying surface and stick there. Once the beam touches the ground plate, an area of contact is the result of a second and final balance between electrostatic and mechanical forces. A number of elaborate and detailed numerical investigations have been dedicated to this and similar systems. The cusp singularity [5] further complicates the analysis. We are not interested in the precise dynamics, and treat the system as singular: it jumps from one static state to another. A recent paper [6] does present a model for the pull-in voltage of a beam with fixed ends, whereas for the μWalker case one end moves freely. Furthermore, no stick region was taken into account in [6], which is essential to determine the step size, in the case of the μWalker. Especially the stick region is of major importance for hysteresis analysis and thus for calculating total energy losses and optimizing the design. A tractable, analytical model for both the electrostatic and elastic domains is derived. Various aspects of the beam motor are analyzed, such as hysteresis and design parameter dependencies. The beam inertia dynamics has been omitted here; mass effects and vibrations are not expected to have a major impact on the results. These effects can be coped with and implemented later on, in numerical studies of a refined model. Finally, the model is compared to measurements of the μWalker.

The working principle of the μWalker is based on the caterpillar's moving principle. Variation of the device output force is accomplished by changing the electrostatic forces applied. These forces are a result of voltage variations

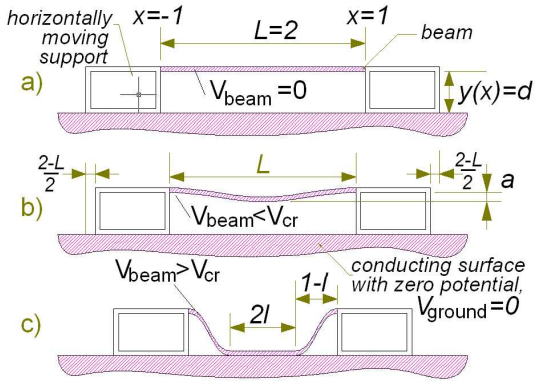

Fig. 2. The creeper beam is in either of the three modes:
a) at rest while no voltage applied ($V_{beam} = 0$);
b) in free mode, due to an applied voltage below the critical voltage ($V_{beam} < V_{cr}$);
c) in stick mode due to a voltage V_{beam}, where $V_{beam} > V_{cr}$.

applied to the three distinct inputs, namely two for the supports and one for the beam. Let us assume that the device has to complete one step to the right. In the start position, only the right support is clamped by an applied voltage. The left support is free to move sideways. Next, the beam voltage is increased, such that the distance between the supports decreases by one step size. The left support is now clamped, while the right support is released shortly thereafter. The beam voltage is lowered and the beam relaxes. This completes one cycle of the μWalker. For more details, see Figure 2.

2 Elastic Part

The system of a creeper beam has bending or elastic energy and electrostatic energy, which are treated in this and the next section respectively. The beam profile is assumed to be a function of a single parameter for the beam deflection, a, where $a < d$ and d is the distance between the beam and the contact surface. (See Figure 2(a,b).) In a variational approach, where the minimum energy is determined for the beam profiles, the solution is an upper bound for the energy, and the typical pitfalls of nonlinear differential equations are avoided. The profiles are a function of a single parameter a, which is the distance from the rest position to the center of the beam, namely at $x = 0$:

$$y(x) = d - a(1 - x^2)^2 \quad , \tag{1}$$

where $y(x)$ is the vertical deflection, and $x \in [-1, 1]$ is the reference coordinate. Throughout the paper, the results are expressed in terms of the units of half of the length of the beam $L_0 = 2$, and energies are in units of energy per width of the beam w, since both the elastic and the electrostatic energy scale linearly with the width of the beam. In this way, the equations are easier to

follow. Only at the end, the value of L_0 is set equal to the real beam length of the $\mu Walker$.

From numerical studies [7], the profile chosen has an appropriate shape, given the clamped boundary conditions. Even if small deviations of the beam shape occur, their influence on the energy is only of second order and negligible. The energy functional has an elastic and an electrostatic part which are determined below.

In simple beam models like the Euler-Bernoulli beam, only the vertical displacement y as a function of the horizontal rest, or reference coordinate x is determined. In our case, the horizontal displacement is also important for the walking motion. The length of the beam is taken to be fixed in the absence of stress through friction. Therefore, the horizontal position $X(x)$ as function of the reference coordinate x should satisfy:

$$1 = (\partial_x X(x))^2 + (\partial_x y(x))^2 \quad ,$$

which is satisfied to second order in a by:

$$\partial_x X(x) = 1 - \frac{1}{2}(\partial_x y(x))^2 = 1 - 8a^2(1-x^2)^2x^2 \quad ,$$

where is assumed that $|1 - \partial_x X(x)| \ll |\partial_x y(x)|$, since $a \ll 1$. The horizontal distance L between the ends at $x = -1$ and $x = 1$ is therefore given by:

$$L = \int_{-1}^{1} \partial_x X(x) dx = 2 - \frac{128}{105}a^2 \quad . \tag{2}$$

The bending energy E_b of a fixed length beam is a function of the beam curvature k[8]:

$$E_b = \int_{-1}^{1} \frac{\kappa}{2} k^2(x) dx \quad ,$$

where the constant κ is given by:

$$\kappa = EI \quad ,$$

and for the curvature k holds:

$$k(x) = \partial_x y(x) \partial_x^2 X(x) - \partial_x X(x) \partial_x^2 y(x) \quad ,$$

since the beam length is a unit function of x. For the given profile, this reduces to the Euler-Bernoulli result [9]:

$$k(x) \approx -\partial_x^2 y(x) = -4a(1 - 3x^2) \quad ,$$

$$E_b = \kappa \frac{64}{5} a^2 = \frac{64}{5} EI a^2 \quad , \tag{3}$$

where E is Young's elasticity modulus, and I the moment of inertia in the direction of bending, which equals $b^3/12$, where b is the beam thickness. Note that both the elastic and the electrostatic energy are proportional to the width of the beam. Therefore, the energy is expressed per unit width.

Of course it is possible to have a more elaborate model of the energy, including higher-order terms in a. However, for qualitative results they are of little consequence, as we will see. Furthermore, given the simple one-parameter ansatz for the beam profile, the approximations are within the same order.

3 Electrostatic Part

The beam itself is a conductor, therefore inside the beam the electric field is zero. For a given potential, the electric field $E_\parallel(x)$ between the beam and the floor is given by the voltage V divided by the distance between beam and floor $y(x)$:

$$E_\parallel(x) = \frac{V}{y(x)} \quad .$$

Since $d \ll L$, we assume the perpendicular component of the electric field $E_\perp$, pointing in the horizontal direction, to first approximation to be negligible. The electric field is the consequence of the surface charge density $\rho(x)$ which is consequently proportional to the strength of the field [10]:

$$\rho(x) = \epsilon_0 E_\parallel(x) \quad .$$

Later, it will be shown that the parallel field approximation holds for all physical configurations. For small values of a, if $d \ll L$, the curvature is small and the beam shape is almost flat. Since large values of a, ($a > d/2$) are not stable, those configurations will not occur and when the beam sticks to the ground plate, the electrostatic energy is dominated by the sticking part. In the case of stick, the gap field, parallel or not, can be neglected. In Figure 3 the equipotential lines of a very short beam at a very large deflection are shown. Even in that extreme case the field is almost parallel. In practice, in this case the beam will stick to the ground floor. In the operational practice the supports may have different voltages compared to the beam, however, this will have neglible effects for the typical flat configuration, where $d \ll L$.

The total electrostatic energy E_e can be expressed as:

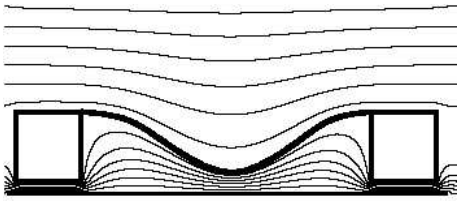

Fig. 3. The equipotential lines from a numerical study of a very short beam at large deflection shows the leading non-perpendicular effects of the beam deflection on the field.

$$\begin{aligned} E_e &= \frac{\epsilon_0}{2}\int_{-1}^{1} y(x)\partial_x X(x) E_{\parallel}^2(x) dx \\ &= \frac{\epsilon_0 V^2}{2}\int_{-1}^{1} \partial_x X(x)\frac{1}{y(x)} dx \\ &\approx \frac{\epsilon_0 V^2}{2}\int_{-1}^{1} \frac{1}{y(x)} dx \quad , \end{aligned} \tag{4}$$

where $y(x)\partial_x X(x)dx$ is the area of the gap, and $\epsilon_0 E_{\parallel}^2(x)/2$ its energy density. The integral is a little tedious to solve. Clearly, the result is dominated by $x \approx 0$. The integrand can be expanded:

$$\frac{1}{d - a(1-x^2)^2} = \frac{1}{r(x^2 + \Delta - 1)} - \frac{1}{r(x^2 - \Delta - 1)} \quad ,$$

with $r = 2\sqrt{ad}$ and $\Delta = \sqrt{d/a}$. The electrostatic energy is therefore given by:

$$E_e = \frac{\epsilon_0 V^2}{r}\left(\frac{\arctan\frac{1}{\sqrt{\Delta-1}}}{\sqrt{\Delta-1}} + \frac{\operatorname{artanh}\frac{1}{\sqrt{\Delta+1}}}{\sqrt{\Delta+1}}\right) \quad .$$

For the sake of model tractability, the electrostatic energy is well fitted with a simple squareroot singularity:

$$E_e = \frac{\epsilon_0 V^2}{2d}\left(2.2\left(\frac{1}{\sqrt{1-\frac{a}{d}}} - 1\right) + 2\right) \quad .$$

Figure 4 reveals that the energy is fairly constant for a large range of a. Therefore, within that range, the actual value of a cannot be determined accurately for a given voltage. The results will depend on the details of the beam shape, and minor differences in the fabrication process and the experiment. However, as shall be seen later on in Figure 9, this is of little consequence for the correct dynamical behavior, as the beam will reach the critical bending a well before $a = 0.5d$, after which it will stick to the floor. Note again that the dynamics and time scale of this motion have not been considered.

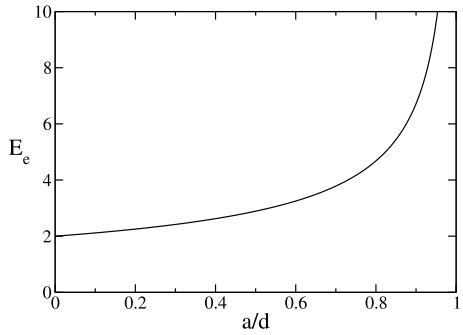

Fig. 4. The normalized electrostatic energy, $\epsilon_0 V^2/2d = 1$.

4 Electroelastic Part

The electrostatic and the elastic part are the opposite forces assumed to act on the beam. The applied voltage difference puts opposite charges close together, such that they attract, decreasing the electrostatic energy as the beam bends and the charges come closer together. The balance can be determined from combining the two in a single electroelastic energy. The energy functional depends on the voltage and the distance a. For each voltage there is an energy profile, as a function of the bending a, in which there exists a local minimum if:

$$0 = \frac{\partial E_b - E_e}{\partial a} = \frac{128}{5}\kappa a - \frac{\epsilon_0 V^2}{4d^2} 2.2(1 - \frac{a}{d})^{-\frac{3}{2}} \quad .$$

Only the local minima $a_{\min}(V)$ need to be determined. Note that this corresponds to a fifth-order polynomial in a, for which there is no closed analytical solution. However, it is straightforward to determine the critical voltage for which a local minimum of the energy exists:

$$V^2 = 46.5\kappa d^2 a \left(1 - \frac{a}{d}\right)^{\frac{3}{2}} \quad ,$$

which has a maximum for $a = 2d/5$:

$$V_{cr}^{+} = \sqrt{\frac{8.65\kappa d^3}{\epsilon_0}} \quad . \tag{5}$$

Often, V_{cr}^{+} is also called the pull-in voltage in the literature. Since for $a > 2d/5$ there is no stable minimum anymore, the parallel field approximation is justified for the case of a gap between the beam and the ground plate, since the gap is large.

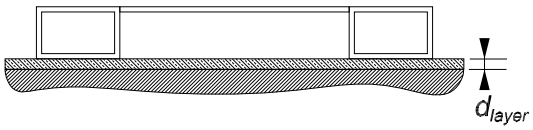

Fig. 5. The surface now also consists of an insulation layer of thickness d_{layer} and with permittivity ϵ_r.

5 Stick

When the beam hits the floor, it will stick there. (See Fig. 2(c).) In practice, a small insulating layer exists with electric permittivity ϵ_r, which prevents charge displacement between the beam and the surface in case there is contact. (See Figure 5.) This situation is entirely different from the free beam of the previous section, and determined mainly by the properties of the stick. First, the energy associated with stick is determined. Second, the configurations are parametrized by the size of the contact length l.

The distance h between the beam and the conduction floor is an effective thickness, which combines the electric permittivities of the airgap and the insulating layer:

$$h = d + \frac{d_{\rm layer}}{\epsilon_r} = d(1+\delta) \quad ,$$

where $\delta \ll 1$. The corresponding energy is referred to as the stick energy E_s and can be obtained from the energy density D_s:

$$\begin{aligned} D_s &= \frac{\epsilon_0 V^2}{2d\delta} \quad , \\ E_s &= 2lD_s \quad . \end{aligned} \tag{6}$$

As can be seen in Figure 2(c), the configuration is thus extended beyond $a = d$ by including a stick domain of length $2l$, and two bending domains, each of the length $1 - l$. The bending energy can be determined from the free case. The two ends can be glued together to yield the $a = d$ case, with scaled $x \to x/(1-l)$ coordinates. The bending energy scales appropriately:

$$E_b^{\rm stick}(l) = \frac{1}{(1-l)^3} E_b(a=d) = \frac{64\kappa d^2}{5(1-l)^3} \quad .$$

The electrostatic energy of the bending part scales with the area:

$$\begin{aligned} E_e^{\rm stick}(l) &= (1-l)E_e(a=d) \\ &= (1-l)\frac{\epsilon_0 V^2}{d}\left(\frac{1.1}{\sqrt{\delta}} - 0.1\right) \quad . \end{aligned} \tag{7}$$

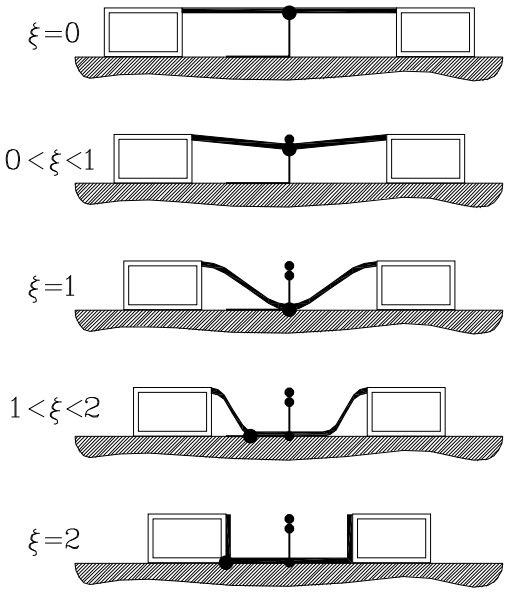

Fig. 6. A sketch of the configuration variable ξ. The vertical path is the distance between the beam and the floor, at $\xi = 1$ the beam touches the floor, the horizontal path is the edge of the contact area.

The total energy of the stick situation is given by:

$$E^{\text{stick}} = E_b^{\text{stick}}(l) - E_e^{\text{stick}}(l) - E_s \quad . \tag{8}$$

The minimum energy is given through the variation with respect to l, where the $E_e^{\text{stick}}(l)$ term is assumed to be of small importance since $\delta \ll \sqrt{\delta}$. The analysis presented in [11] confirms this. The length of the stick area, for the minimum energy:

$$l_{\min} = 1 - \sqrt[4]{\frac{192\kappa d^3\delta}{5\epsilon_0 V^2}} \quad .$$

If $l_{\min}$ is real negative, then the beam will stick at the boundary point, $l_{\min} = 0$. This situation occurs, since the first derivative of the energy kinks downwards at the cross-over between stick and free mode, creating a cross-over minimum, since in each domain, stick and non-stick, the boundary value is a local minimum.

The distance between the beam ends changes further as the stick area increases. In principle it would scale with $(1-l)^{-1}$, however, for values of $l \to 1$, the approximation fails. The corrected length incorporates this effect:

$$L = 2 - \frac{128}{105}\frac{d^2}{1-(1-\frac{64}{105}d)l} \quad ,$$

yielding a minimal distance of $L_0 - 2d$ for $l = 1$, where $L_0 = 2$ is the beam

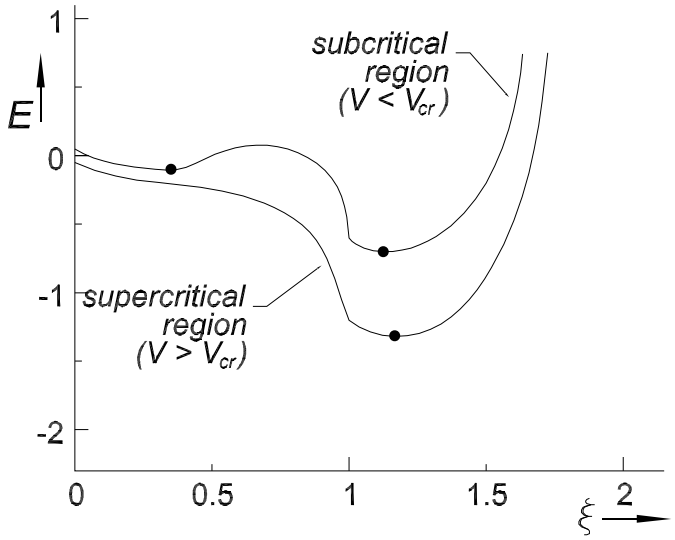

Fig. 7. A sketch of the energy as function of the configuration variable ξ and the potential for sub- and supercritical values of the potential.

length at rest. However, once the beam touches the ground, it might create a rigid construction, such that the whole or half of the beam does not move further. In practice, one could think about cold welding points and stick due to certain material properties.

For a complete model, we now introduce a single configuration variable ξ, $0 < \xi < 2$, to be valid in all three modes (see Figure 2). Figure 6 illustrates this:

$$\xi = \begin{cases} \xi < 1: \quad \xi = \frac{a}{d}, \quad \text{if} \quad l = 0 \quad , \\ \xi > 1: \xi = 1 + l, \text{ if} \quad a = d \quad . \end{cases} \tag{9}$$

In Figure 7, two possible solutions for the electroelastic energy have been plotted as a function of ξ. The upper solution is called a subcritical region, while the lower is called supercritical region. It is clear that there are two minima for the subcritical region, while there is only one minimum for the supercritical region. From Eq. 5, V_{cr} is the border between the two regions. How the system will jump from the disappearing local minimum to the absolute minimum depends on the characteristics of the voltage source, damping coefficients, and the distributed mass of the beam. For our purpose, however, the jump is assumed to be instantaneous without loss of generality.

The electroelastic energy can be expressed in ξ as for both the sub- and supercritical potential values, respectively:

$$E_<(\xi, V) = \frac{1}{2}K\xi^2 - \frac{1}{2}CV^2\frac{1}{\sqrt{1+\delta-\xi}} \quad , \tag{10}$$

$$E_>(\xi, V) = \frac{1}{2}\frac{K}{(2-\xi)^3} - \frac{1}{2}CV^2\frac{1}{\delta}(\xi - 1 + \sqrt{\delta}) \quad , \tag{11}$$

where $C = \frac{2\epsilon_0\sqrt{1+\delta}}{h}$ is the electric capacity and $K = \frac{32}{5}EId^2$ is the normalized mechanical bending stiffness, see Eq. 3. The small constant terms were disregarded.

In the case of absolute units, there holds:

$$C = w\frac{L_0\epsilon_0}{d\sqrt{1+\delta}} \quad , \tag{12}$$

$$K = \frac{32EId^2}{5L_0^3} = w\frac{64}{15L_0^3}Eb^3d^2 \quad , \tag{13}$$

where L_0 is the length of the beam, and b the thickness of the beam. The moment of inertia is given as:

$$I = \int_{\frac{1}{2}w}^{\frac{1}{2}w} dy \int_{\frac{1}{2}b}^{\frac{1}{2}b} z^2 dz = \frac{wb^3}{12} \quad .$$

The absolute scaling of the model shows that C scales linearly with size and K with the cube of the size, such that the critical voltage scales linearly with size (See Eq. 5.) Hence, a smaller system requires an equally smaller working voltage.

6 Point Stick and Hysteresis

Point stick is a local minimum of the energy function at $\xi = 1$, if the left-derivative of the energy profile is negative and the right derivative is positive. In this case, the beam will touch the ground plate at a single point. This situation occurs for

$$\frac{4K\delta^{\frac{3}{2}}}{C} < V^2 < \frac{3K\delta}{C} \quad .$$

Therefore the critical jump-back voltage for the situation from stick-to-free is the lower bound of the point stick:

$$V_{cr}^- = \sqrt{\frac{4K\delta^{\frac{3}{2}}}{C}} \quad .$$

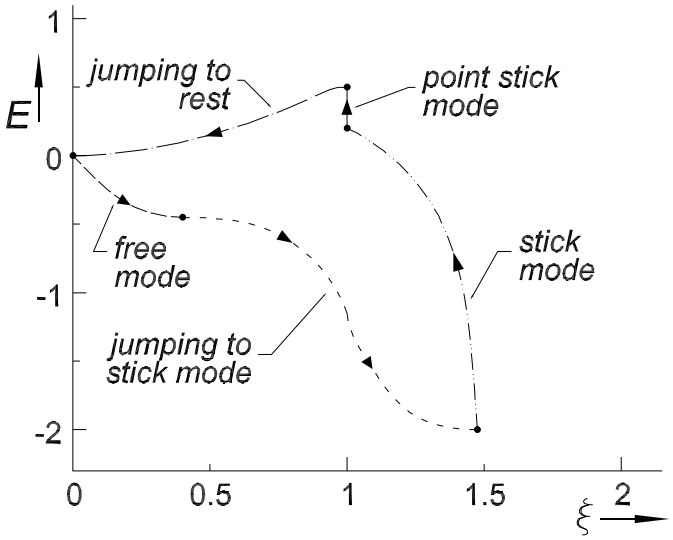

Fig. 8. Trajectory for certain design parameters and applied voltage.

The energy at the critical point is:

$$E_{\max} = \frac{1}{2}K(1-2\delta) \quad .$$

As shall be presented shortly, this corresponds to the vertical segment in Figure 9. In the situation where the voltage is increased above the upper critical value V_{cr}^{+}:

$$V_{cr}^{+} = \sqrt{\frac{8K(1+\delta)^{\frac{5}{2}}\left(\frac{3}{5}\right)^{\frac{3}{2}}}{5C}}$$

and then lowered again till below the lower critical value V_{cr}^{-}, the system will make a loop in the configuration space. Figure 8 shows a possible loop, that the system will walk through, for a certain applied voltage as a function of time. Let us distinguish five domains:

(1) Free mode: As the voltage increases and the beam bends due to the electrostatic force, there is a balance between the bending and the electrostatic energy.
(2) Jump to stick: At the given voltage V_{cr}^{+}, the electrostatic energy dominates the bending energy; the system jumps suddenly towards the stick mode with a contact area.
(3) Stick mode: Because of decreased voltage, the stick area decreases until it approaches zero length.
(4) Point stick mode: The beam sticks at one point, until the voltage decreases below V_{cr}^{-}.
(5) Jump to rest: The system instantaneously jumps to the rest position.

In the case of the stick mode, the voltage can be lowered even further, the

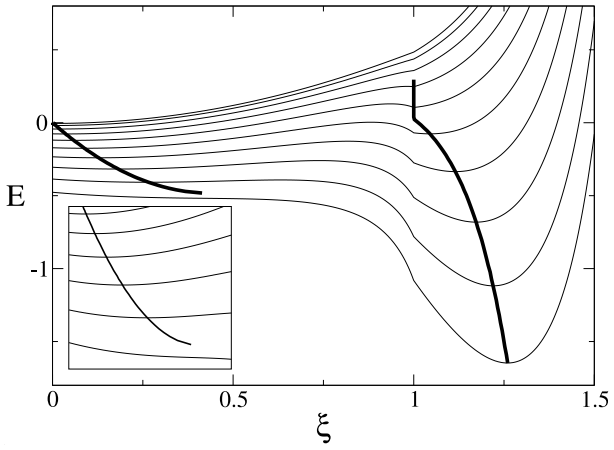

Fig. 9. The trajectories of the system indicated through the two line segments, the left one for increasing voltage (going into stick mode), the right one for decreasing voltage (releasing from stick mode).

stick domain indicated by $\xi > 1$ will then decrease. The value of ξ for which the energy acquires a minimum for a given voltage is given by:

$$\xi = 2 - \sqrt[4]{\frac{3K\delta}{CV^2}} \quad .$$

The corresponding energy follows from the virial theorem:

$$E_{\min} = -\frac{(3^{\frac{1}{4}} - 3^{-\frac{3}{4}})K^{\frac{1}{4}}C^{\frac{3}{4}}V^{\frac{3}{2}}}{2\delta^{\frac{3}{4}}} + \frac{1}{2}CV^2(1-\sqrt{\delta}) \quad .$$

As an aggregation, Figure 9 shows one of several possible system trajectories, depending on physical parameters. The left segment represents the beam for increasing voltage starting at $V = 0$, where the beam is stuck in the bend minimum. The right part is for decreasing voltage, when the system is stuck in the stick minimum. The vertical segment indicates the point contact sticking. The zoom-in shows that there is indeed a flat minimum, which disappears below a certain energy profile, and thus the local minimum also disappears. Formally, at this point (ξ_{cr}) holds:

$$\left.\frac{\partial E\left(\xi\right)}{\partial \xi}\right|_{\xi \downarrow \xi_{cr}} = \left.\frac{\partial^2 E\left(\xi\right)}{\partial \xi^2}\right|_{\xi \downarrow \xi_{cr}} = 0 \quad .$$

The energy loss in the system during a cycle is associated with the two jumps, when the voltage crosses the two critical values V_{cr}^{+} and V_{cr}^{-}. The down jump

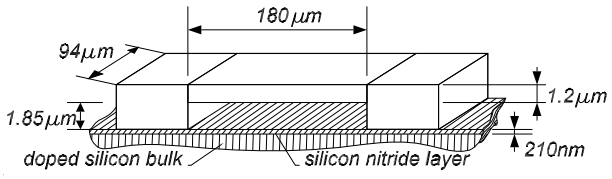

Fig. 10. The μWalker dimensions assumed.

corresponds to an energy jump ($\xi = \frac{2}{5}(1+\delta) \rightarrow \xi = 2 - \sqrt[4]{3K\delta/CV_{cr}^{+2}}$):

$$\Delta E_{\downarrow} = E_{\min}(V_{cr}^{+}) - \frac{2K(1+\delta)^2}{25} + \frac{CV_{cr}^{+2}}{2\sqrt{\frac{3}{5}(1+\delta)}} \quad ,$$

while the up jump corresponds to an energy jump ($\xi = 1 \rightarrow \xi = 0$):

$$\Delta E_{\uparrow} = E_{\max} = \frac{1}{2}K(1-2\delta) \quad .$$

Thus, the total energy needed for one cycle equals:

$$E_{tot} = \Delta E_{\downarrow} + \Delta E_{\uparrow} \quad .$$

7 The μWalker - a case

As a test case, a design similar to the μWalker is presented in [2]. The bulk material is Silicon (Si), whereas the insulation layer consists of Silicon nitride (SI_RN). The Silicon nitride has a dielectric constant in the range of 5 to 8, and a dielectric strength of about $1.0 - 2.0\ 10^8 V/m$. In the case of voltages below $100V$, a layer of $1.0\mu m$ is sufficient for reaching the stick phase. However, in the case of the μWalker, the bottom surface is specially prepared for enhancing sliding properties. The thickness of the dielectric layer is $0.210\mu m$, but the effective thickness is much larger than the corresponding $\delta = 0.03$, due to the prepared contact area of the beam with small pins of about the same height. The small pins create an airgap when the beam hits the ground plate. The original design, without pins, stuck to the ground plate, even after the voltage was decreased. This was the result of large stick energy, due to the small value of δ. Although, we have not been able to determine δ accurately from the design, the size of the pins suggests an effective Silicon-nitride-air layer of around $\delta = 0.2$, which is mainly due to the large airgap. This value can experimentally be obtained from the step size.

The length L_0 of the beam is $180\mu m$ and the distance d to the floor is $1.85\mu m$. Figure 10 shows the dimensioning assumed. The width of the beam is $94\mu m$, which justifies the parallel field approximation in the third direction. The beam itself has a thickness of $1.2\mu m$, which corresponds to a moment of inertia of

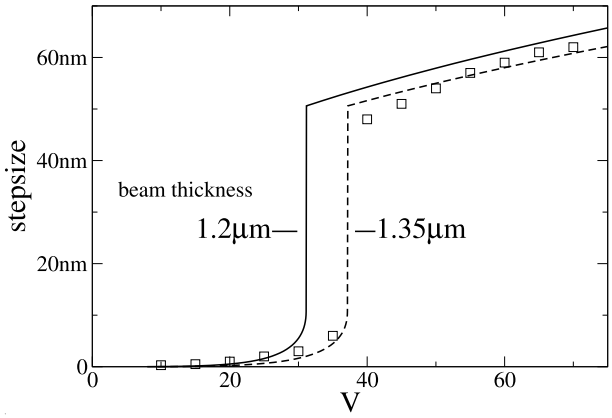

Fig. 11. The squares are the measured step sizes. The solid line is the step size from the model. The dashed line is the step size for the adjusted beam thickness of $1.35\mu m$.

$I = 1.35\ 10^{-23} m^3$. For an Young's modulus of $E \approx 150\ 10^9 Pa$, Equations 12 and 13 give:

$$K = 6.1\ 10^{-11}\mathrm{Nm}^{-1} \quad , \tag{14}$$

$$C = 7.4\ 10^{-14}\mathrm{F} \quad . \tag{15}$$

According to the model proposed, the upper critical voltage $V_{cr}^{+} \approx 31V$, while the lower critical voltage $V_{cr}^{-} \approx 17V$. The maximal displacement in a single cycle is about 50 nm, if it is assumed that half of the beam is fixed once it touches the ground plate, while the other half still pulls inward. In Figure 11 some measured step sizes of the μWalker are plotted together with the results of the model presented, including the parameters from above. The results depend strongly on the thickness of the beam. A slight adjustment of the beam thickness from $1.2\mu m$ to $1.35\mu m$ would diminish the small discrepancy in the pull-in voltage between the model and the measurements, as can be seen in the figure. The results depend only weakly on the effective layer thickness δ. A smaller delta would increase the step size, but would leave the pull-in voltage the same.

8 Conclusions

For the sake of simplicity, dynamical effects were ignored throughout the paper. In principle, the system will stay in the local energy minimum if the changes are infinitely slow. If the changes occur faster, the system will build up inertia, which could lower the energy barriers and the pull-in voltage. Furthermore, if the kinetic energy is not enough to jump the barrier, the system will start to oscillate around the minimum. In fact, the point stick situation

will quickly disappear due to dynamical effects. From Figure 9 it is clear that for values of ξ slightly smaller than 1, the system will slide back to $\xi \approx 0$, if the voltage is relatively low. This can also be observed in practice.

The model presented identifies the relevant parameters of the creeper-beam system: the stiffness K, the capacity C, and the insulator thickness δ. Especially the latter is seldom mentioned as an important design parameter for the stick regime. The precise numerical coefficients play a secondary role in finding the analytical dependence of several quantities on the design parameters. Furthermore, the model gives a clear handle on the different dynamical regimes, and identifies a third configuration regime, namely the point-contact stick, for a range of applied voltages. In a more elaborate model, where the bending is not simply modeled by a single parameter, this could be further investigated. However, the scope of this paper is limited to quantify the main features of the creeper beam model, such that the relevant parameters and their effects are identified.

For a model with only one parameter that has been fitted to experiments, namely δ, the results compare very well to the measurements. Moreover, it can be used to fit the data using the three parameters K, C, and δ, such that different properties relevant for design, such as step size, deformation, and force can be compared. As has been remarked in Section 5, smaller dimensions of the beam imply smaller working voltages.

It should be mentioned that friction between the supports and the ground plate may cause stresses in the beam which reduce the step size. In this case the beam will act as a spring rather than fixed-length, bending beam. The dynamical effects – for example as a result of beam inertia – will limit the operation speed since the mechanical effects do not occur instantaneously with the change of the voltage. All these effects are under investigation, both in numerical as well as in experimental studies. However, the simple model presented here has been the guiding principle, as it covers the dominant behavior of the electroelastic beam.

Future work will include 20-SIM modeling of the μWalker as a complete system including stick-slip, friction and other effects that play a great role in the ever interesting world of micro and nano devices.

9 Acknowledgments

The authors would like to thank E. Sarajlic and the μSPAM group for the experimental data. This work was sponsored by STW through projects TWI.6012 and TES.5178.

References

[1] M. J. Madou, Fundamentals of Microfabrication – The Science of Miniaturization, 2nd Edition, CRC Press, (London 2002), ISBN 0-8493-0826-7

[2] T. Lammerink, M. Elwenspoek, L. Sander, J. Wissink and N. Tas, Modeling, Design and testing of the electrostatic shuffle motor, Sensors and Actuators A **70** (1998) pp. 171-178.

[3] M. Bolks, F. Hanssen, L. Abelmann, P. Havinga, P. Hartel, P. Jansen, C. Lodder, G. Smit, Micro Scanning Probe Array Memory (μSPAM), Proceedings second Progress workshop, Veldhoven, the Netherlands, pp. 17-26, ISBN 90-73461-26-X, October 2001.

[4] P. Vettiger, G. Cross, M. Despont, U. Drechsler, U. Uürig, B. Gotsmann, W. Häberle, M. A. Lantz, H. E. Rothuizen, R. Stutz, and G. K. Binning, The "Millipede" – Nanotechnology Entering Data Storage, IEEE Transactions on Nanotechnology **1**, June 2002.

[5] V. I. Arnold, *Catastrophe theory*, Springer (Berlin, 1984). T. Poston and I. Stewart, *Catastrophe theory and its applications*, Pitman (San Fransisco, 1978).

[6] H. Rong, Q. A. Huang, M. Nie, W. Li, An analytical model for pull-in voltage of clamed-clamped multilayer beams, Sensors and Actuators A **112** (*in press*).

[7] Y. Zhou, X. Yang, Numerical analysis on snapping induced by electromechanical interaction of shuffling actuator with nonlinear plage, Computers and Structures **81** (2003) pp. 255-264.

[8] H. W. Guggenheimer, *Differential geometry*, McGraw-Hill (New York, 1963).

[9] A. E. H. Love, *A treatise on the mathematical theory of elasticity*, Dover (New York, 1927).

[10] J. D. Jackson, *Classical electrodynamics*, Wiley (New York, 1962).

[11] Mallon J.R., F. Pourahmadi, K. Petersen, P. Barth, T. Vermeulen, J. Brezek, Low pressure sensors employing bossed diaphragms and precision etch-stopping, Sensors and Actuators A **21-23** (1990) pp. 89-95.

- **Norbert E. Ligterink** received the M.Sc. in Theoretical Physics with honors (cum laude) in 1992 and the Ph.D. in Theoretical Nuclear Physics in 1996. Thereafter he worked at UMIST in Manchester, UK, at ECT*, in Trento, Italy, and at the University of Pittsburgh, USA, on the field-theoretical description of nucleonic and sub-nucleonic bound states. Since 2003 he is a graduate student again. The topic of his Ph.D. is the modeling and control of distributed parameter systems.
- **Mihai Patrascu** received his M.Sc. in 2002 at the Delft University of Technology. He now is a Ph.D. student at the University of Twente, the Netherlands. His interests lie in physical modeling and simulation of micro electro-mechanical systems and new data storage concepts.
- **Peter C. Breedveld** is an associate professor with tenure at the University of Twente, Netherlands, where he received an M.Sc. in 1979 and a Ph.D in 1984. He has been a visiting professor at the University of Texas at Austin in 1985 and at the Massachusetts Institute of Technology in 1992-1993. He is or has been a consultant for several large industrial research labs. He initiated the development of the modeling and simulation tool that is now commercially available under the name 20-sim. In 1990 he received a Ford Research grant for this work in the area of physical system modeling and the design of computer aids for this purpose.

  He is an associate editor of the 'Journal of the Franklin Institute', SCS 'Simulation' and 'Mathematical and Computer Modeling of Dynamical Systems'. His scientific interests are: integrated modeling, control and design of physical systems; generalized thermodynamics; simulation, analysis and design; numerical methods, applied electromagnetism and many more.
- **Stefano Stramigioli** received the M.Sc. with honors (cum laude) in 1992 and the Ph.D with honors (cum laude) in 1998. Since 1998 he has been faculty member first as assistant and then associate professor. He is currently an officer and Senior Member of IEEE. He has more than 60 publications including a book. He is Editor in Chief of the IEEE Magazine of Robotics and Automation, and has been guest editor for others. He is a member of the ESA Topical Team on Dynamics of Prehension in Micro-gravity and its application to Robotics and Prosthetics. He is involved in different projects related to Control, Robotics and MEMS and coordinator of the European Project named Geoplex (http://www.geoplex.cc). He has been teaching Modeling, Control and Robotics for under and post-graduates and received teaching nominations and an award.

FIGURE CAPTIONS

(1) One dimensional version of the μWalker used for modeling and simulation.

(2) The creeper beam is in either of the three modes:
a) at rest while no voltage applied;
b) in free mode, due to an applied voltage below the critical voltage ($V_1 < V_{cr}$);
c) in stick mode due to a voltage V_2, where $V_2 > V_{cr}$.

(3) The equipotential lines from a numerical study of a very short beam at large deflection shows the leading non-perpendicular effects of the beam deflection on the field.

(4) The normalized electrostatic energy, $\epsilon_0 V^2/2d = 1$.

(5) The surface now also consists of an insulation layer of thickness d_{layer} and with permittivity ϵ_r.

(6) A sketch of the configuration variable ξ. The vertical path is the distance between the beam and the floor, at $\xi = 1$ the beam touches the floor, the horizontal path is the edge of the contact area.

(7) A sketch of the energy as function of the configuration variable ξ and the potential for sub- and supercritical values of the potential.

(8) Trajectory for certain design parameters and applied voltage.

(9) The trajectories of the system indicated through the two line segments, the left one for increasing voltage (going into stick mode), the right one for decreasing voltage (releasing from stick mode).

(10) The μWalker dimensions assumed.

(11) The squares are the measured step sizes. The solid line is the step size from the model. The dashed line is the step size for the adjusted beam thickness of $1.35\mu m$.